THE JOURNAL OF COMPARATIVE NEUROLOGY 273:488-499 (1988)

Acetylcholinesterase Fiber Staining in the Human Hippocampus and Parahippocampal Gyrus

ROBERT C. GREEN AND M-MARSEL MESULAM
Division of Neuroscience and Behavioral Neurology, Beth Israel Hospital and Harvard Medical School, Boston, Massachusetts 02215

ABSTRACT

The AChE fiber distribution within the human hippocampus and parahippocampal gyrus was studied in order to provide normative data for the examination of cholinergic fiberarchitecture in human pathology and to clarify the cytoarchitectonic organization of these structures. A modification of the Koelle method was used to stain temporal lobe serial sections from 6 neurologically normal human brains collected at autopsy.

The hippocampal formation contains some of the densest staining of any cortical area. Regions with the heaviest concentrations of AChE fibers include a thin band along the inner edge of the molecular layer of the dentate gyrus (ml-DG) and parts of the CA2, CA3, and CA4 sectors of Ammon's horn. Staining is of intermediate intensity in the CA1 region. The subiculum (S) is more lightly stained than the CA fields. Staining in the parahippocampal gyrus is generally less dense than in the hippocampal formation. The most conspicuous feature of the human entorhinal cortex (EC) is the AChE-rich fiber patches seen overlapping the stellate cell islands in layer II. An additional band of relatively dense AChE staining is identified in layers IV-V. Prominent AChE-rich polymorphic neurons are present within the hilum of the dentate gyrus.

The CA1/subiculum transition in Nissl preparation is characterized by an oblique interdigitation of CA1 cells. The transition from EC to prorhinal cortex occurs along the medial bank of the rhinal sulcus and is characterized by a band of AChE staining, which slopes obliquely away from layer II until it joins an intermediate pyramidal cell layer. Some comparisons with AChE staining in the monkey were made. The monkey has a similar pattern except in DG, where the intensely AChE staining band along the inner ml-DG is thicker and much more prominent. In comparison to the human, the monkey has more conspicuous AChE staining in the parasubicular region.

Key words: limbic system, anatomy, entorhinal cortex, cytoarchitecture, monkey

Animal studies of the hippocampal formation have sparked considerable interest because of the importance of this structure in the normal mechanisms of learning and memory. The pathologic anatomy of the hippocampus has also been examined in human neurologic disorders such as Alzheimer's disease (Terry and Katzman, '83; Hyman et al., '84; Kemper, '84), epilepsy (Babb and Brown, '87), and amnestic disorders (Horel, '78; Squire, '86; Zola-Morgan et al., '86). One limitation of the human studies to date is the variability with which anatomic nomenclature is applied in descriptions of human neuropathology.

Accepted December 29, 1987.

Address reprint requests to Dr. Robert C. Green, Department of Neurology, Emory University School of Medicine, 401 Woodruff Memorial Building, Atlanta, GA 30322.

Histochemical staining of acetylcholinesterase (AChE) has been a valuable method for tracing the distribution of cholinergic pathways in animals. For example, the loss of AChE staining in the rat hippocampus after lesions of the fimbria (Lewis and Shute, '67) and medial septal nucleus (Mellgren and Srebro, '73) have implicated the septohippocampal pathway as the major source of cholinergic input into the hippocampus. AChE fibers also provide a useful first approximation as a marker for choline acetyltransferase containing pathways in the hippocampus (Fonnum, '70; Matthews et al., '83; Amaral and Eckenstein, '86).

In addition to its relevance as a marker of cholinergic pathways, AChE distribution has been valuable in delimiting neuroanatomic regions, since changes in staining intensity often follow cytoarchitectonic and laminar boundaries. For example, AChE staining has helped to delineate the complex subfields of the hippocampal formation and parahippocampal regions in a number of animal species including the mouse (Vijayan, '79), rat (Mathisen and Blackstad, '64; Mellgren, '73), guinea pig (Geneser-Jensen and Blackstad, '71, Geneser-Jensen, '72a,b), rabbit (Geneser, '86), and monkey (Bakst and Amaral, '84).

Despite its value in animal preparations, AChE staining has been used on a relatively limited basis in the pathologic analysis of human material (Geddes et al., '85; Hyman et al., 87). In part, this may be due to the paucity of systematic studies of the normal distribution of AChE staining in these structures. Reports by Friede ('66) and Mellgren et al. ('77) were limited to the AChE staining of the hippocampus proper. AChE-positive cells were identified in the hilum of the human dentate gyrus by Okinaka et al. ('61), and a brief report by Kelovic and Kostovic ('81) was restricted to the entorhinal cortex.

The present report examines the distribution of AChE fibers in the dentate gyrus, Ammon's horn, subicular complex, and entorhinal region of the human brain. Corellations are made with cytoarchitectonic regions as defined on adjacent sections stained with thionin. Some comparisons with AChE staining in the hippocampus of the monkey are made.

MATERIALS AND METHODS

Tissue from 6 human brains was obtained at autopsy 2–18 hours after death. The left temporal lobe was removed en bloc from a 29-year-old female (ruptured aortic aneurysm) and a 43-year-old male (sudden cardiac death). The right temporal lobe was similarly removed from a 2-year-old female (congenital heart disease, perioperative death), a 13-year-old male (leukemia with sepsis prior to death), a 30-year-old male (liver failure, pneumonia, and sepsis), and a 63-year-old male (lymphoma and sepsis). The tissue was blocked coronally into 2-cm slabs and immersion fixed for 24 hours in a phosphate-buffered solution of 4% paraformaldehyde, followed by 2–3 days in each of 4 increasingly concentrated series of 0.1 M phosphate-buffered 10–40% w/v sucrose solutions (pH 7.4).

Serial coronal sections were cut at 40 μm on a freezing microtome into a 0.1 M phosphate-buffered solution (pH 7.4) and mounted onto chrome-alum subbed slides. After drying for no more than 24 hours at room temperature, several 1-in-25 series of sections were processed for the demonstration of AChE at various incubation times. An adjacent series was always stained by the Nissl method and an AChE stained series was counterstained with thionin.

AChE fiber staining was obtained by a modification of the copper thiocholine method (Koelle and Friedenwald, '49). The incubation medium contained 4 mM acetylthiocholine iodide, 0.2 mM ethopropazine, 2 mM copper sulfate, 10 mM glycine, and 50 mM acetate buffer. Incubation trials were run at a range of pH values from 5.0 to 5.5 until it was determined that fiber staining was best seen. Incubation conditions were at room temperature for 1–4 hours with gentle rocking. After incubation, sections were washed thoroughly in 0.1 M sodium acetate solution, then placed into a 160 mM solution of sodium sulfide for 1 minute. The sections were again washed thoroughly and intensified in a 1% silver nitrate solution before final washing in at least 6 rinses of distilled water, dehydration, and coverslipping. AChE stained sections that were Nissl counterstained were air dried after the final rinse and taken through either thionin or cresyl violet staining in the usual manner. Control sections were processed with 4mM butyrylthiocholine iodide as a substitute for acetylthiocholine iodide, and both substrates were used with and without ethopropazine.

Material was also analyzed from a sample of 3 male and 1 female rhesus monkeys (*Macaca mulatta*) in the adolescent-adult age range. The monkeys were sacrificed and serial 40 μm sections of AChE and Nissl staining were processed as previously described (Mesulam et al., '84). Normal material for cytoarchitectonic study also included human whole brain sections of a 28-year-old human that had been embedded in celloidin, cut at 40 μm, and stained with cresyl violet (Yakovlev, '70).

RESULTS

Staining characteristics and anatomic nomenclature

The AChE procedure yielded a reaction product that resulted in a granular staining pattern over the areas with intense enzyme activity. Over many areas and especially at higher magnifications, clearly stained fibers were also discernible. Regional variations in staining density and morphology were noted throughout the hippocampus and parahippocampal gyrus. The high contrast between stained

Abbreviations

A	amygdala
al	alveus
CA 1–4	fields of the hippocampus
EC	entorhinal cortex
f	fimbria
fds	fimbriodentate sulcus
g	granule cell layer of the dentate gyrus
hs	hippocampal sulcus
I-VI	layers of cortex
lm	stratum lacunosum moleculare
mf	mossy fiber layer (stratum lucidum)
ml-AH	molecular layer of Ammon's horn
ml-DG	molecular layer of the dentate gyrus
o	stratum oriens
p	stratum pyramidale
Pe	perirhinal cortex
Pr	prorhinal cortex
PreS	presubiculum
ProS	prosubiculum
r	stratum radiatum
rs	rhinal (collateral) sulcus
S	subiculum
Se	external layer of subicular pyramidal cells
Si	internal layer of subicular pyramidal cells
tc	tail of the caudate

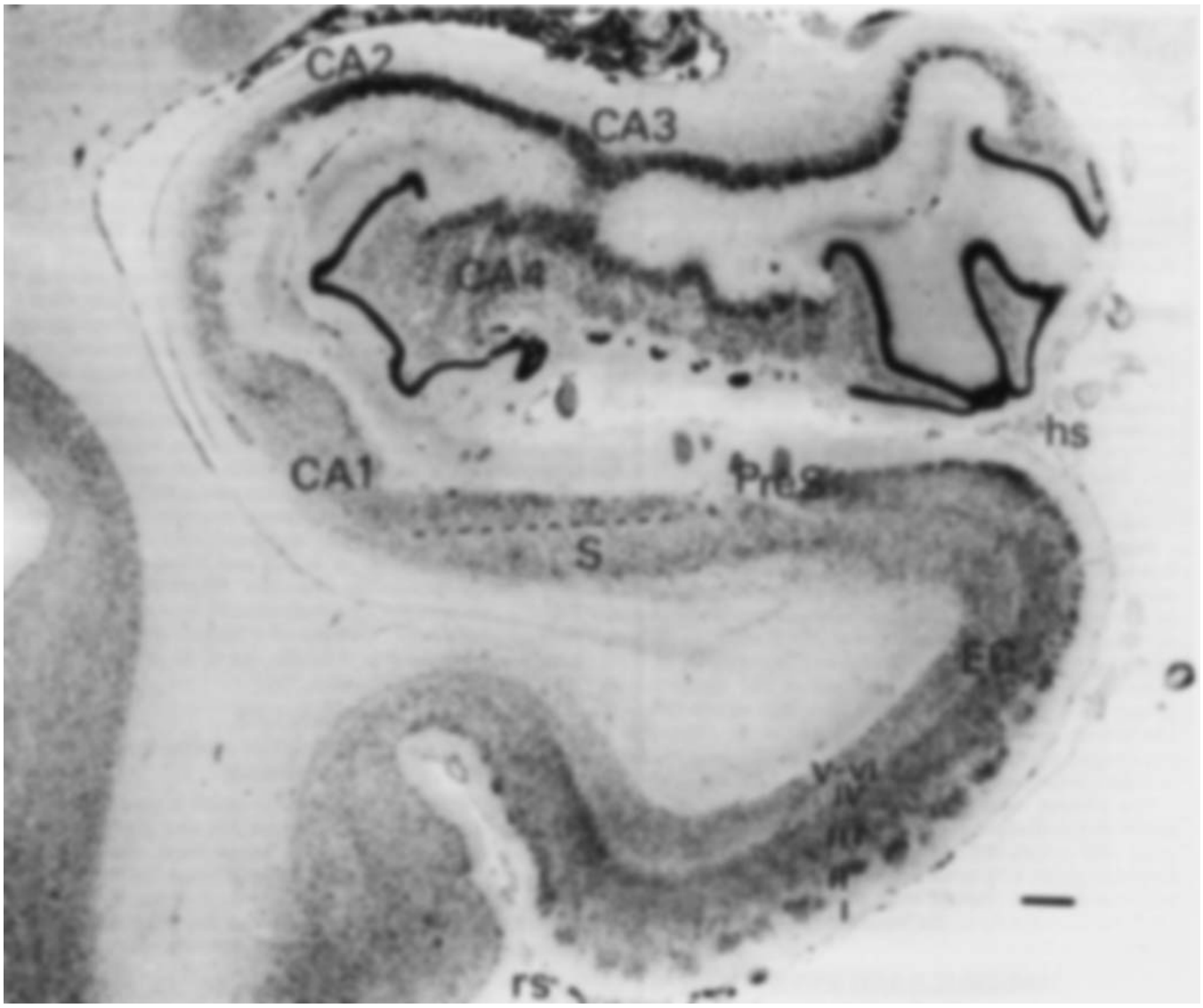

Fig. 1. This celloidin-embedded, Nissl-stained coronal section through the rostral hippocampal formation and entorhinal cortex of a 28-year-old human shows the major architectonic subdivisions. The dotted line marks the division between CA1 and subiculum. Calibration mark = 1 mm.

and unstained regions was useful for defining regional boundaries. Many cerebral areas contain AChE-rich perikarya as well as AChE-rich axons. In this report, we concentrate on the axonal AChE.

We have chosen to follow the descriptions and nomenclature of Lorente de Nó ('34) and Braak ('80). Some areas, especially in the parahippocampal gyrus, have been described in terms of homologous regions in the monkey. Each section on AChE staining is preceded by a brief description of the relevant cytoarchitectonic nomenclature.

The hippocampal formation: Dentate gyrus

Nomenclature. The dentate gyrus, along with Ammon's horn and the subicular complex together constitute the *hippocampal formation*. This terminology has largely supplanted older names such as *pes hippocampus* or *hippocampus major* and *minor*.

Both Ramón y Cajal (1893) and Lorente de Nó ('34) use the term *fascia dentata* to designate the indented layer of cortex that caps or "embraces" the terminal portion of Ammon's horn. This cortical region is formed by an involuted gyrus that is delimited by the hippocampal sulcus including its fused extent on one side, and by the fimbriodentate sulcus on the other. Many contemporary researchers have designated this area as the dentate gyrus, and we use this term exclusively.

The dentate gyrus is composed of 3 layers: the molecular layer, the granule cell layer, and the subjacent polymorphic layer (Ramón y Cajal, 1893). The polymorphic cell layer is impossible to delimit precisely from the neurons of the CA4 field (Figs. 1, 2).

Distribution of AChE. The granule cell layer exhibits relatively little AChE staining, and therefore stands out against the more heavily staining, immediately adjacent

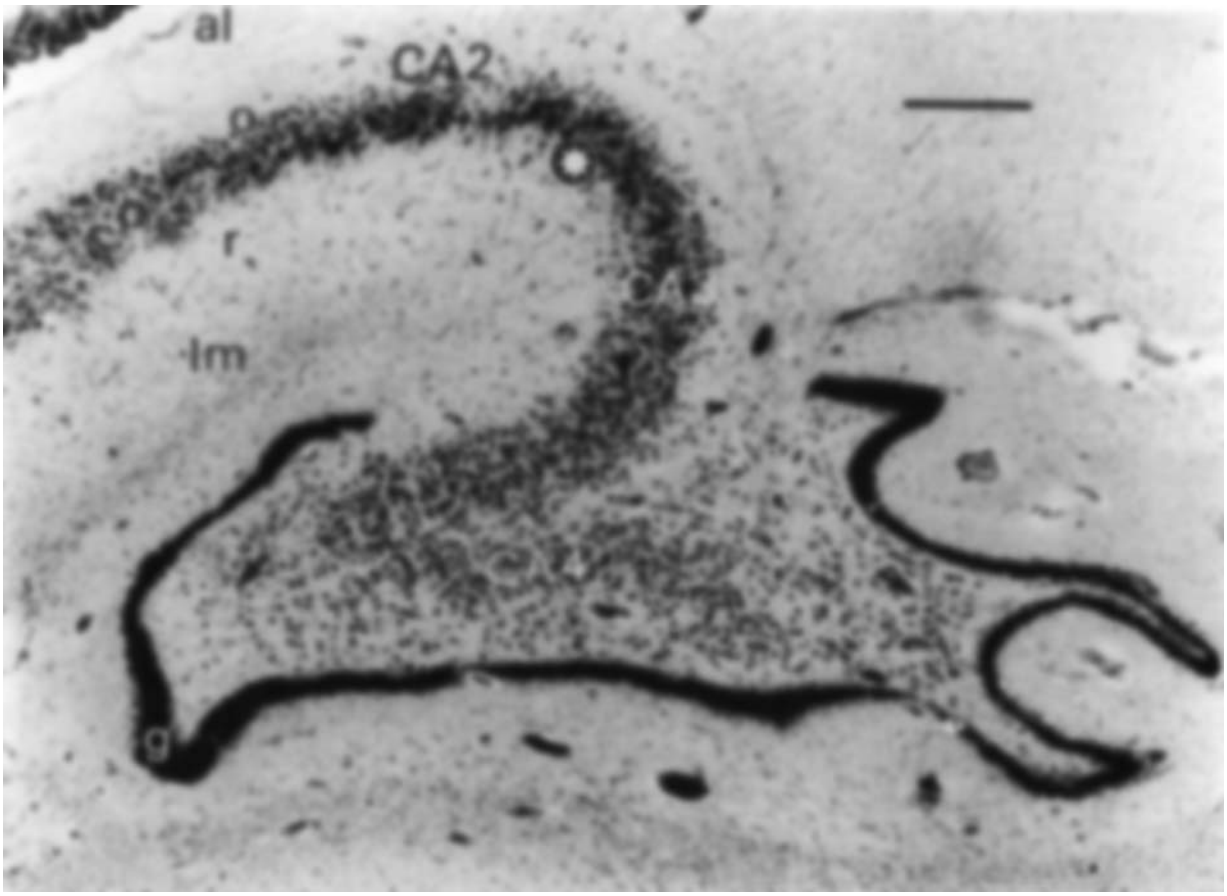

Fig. 2. This celloidin-embedded, Nissl-stained coronal section through the mid-caudal region of a 43-year-old human demonstrates the laminar organization of Ammon's horn and the dentate gyrus. The circular marker overlies the stratum lucidum. The arrows indicate regions of nonpyramidal hilar cells. Many of these endofolial polymorphic cells stain heavily for AChE. Calibration mark = 1 mm.

areas (Figs. 3, 4). Examination of thionin counterstained preparations shows that strands of AChE-positive fibers cross the granule cell region transversely.

In the molecular layer of the dentate gyrus, AChE staining is heaviest along a thin band immediately adjacent to the granule cell layer (Fig. 4). Lighter, fairly homogeneous staining occurs throughout the more superficial parts of the molecular layer. The hilum of the dentate gyrus contains cells that stain prominently for AChE. These are most densely distributed within the outer perimeter of the hilar region and some are immediately subjacent to the granular layer of the dentate gyrus.

The hippocampal formation: Ammon's horn

Nomenclature. Ammon's horn was divided by Lorente de Nó ('34) into the CA1-4 sectors on the basis of Golgi stains. As he points out, the distinction between these sectors cannot always be reliably made by Nissl staining. We designate as CA4 the extension of the stratum pyramidale into the hilum of the DG. In coronal Nissl sections there is usually a clear difference in cell packing density and perikaryal shape that permits a distinction between the more densely packed and homogeneously shaped pyramidal neurons of the Ammonic formation (i.e., CA4) and the more polymorphic neurons of the DG.

The pyramidal cells of CA2 and CA3 are both characterized as "giant" by Lorente de Nó, and they are distinguished in Golgi stains by the presence in CA3 of long dendritic shafts corresponding to the mossy fiber zone and Schaffer collaterals. Nissl preparations do not demonstrate precise borders between CA3 and CA2, although CA2 is generally characterized by a thinner, more densely packed, and more hyperchromic band of cells in the pyramidal layer (Fig. 2).

The CA1 region largely corresponds to what is also known as Sommer's sector. This region dramatically increases in size with phylogenetic progression (Stephan, '83). The division of the stratum pyramidale into two layers of pyramidal cells is most prominent in CA1 (Fig. 1). The more superficial of these layers in CA1 gradually narrows as it extends over the subicular region. The transitional zone between the CA sectors and the subiculum is discussed in greater detail below.

The CA sectors of the hippocampal formation are further characterized by several laminae. Starting at the ventricular surface in the CA3-2 sector is the alveus, stratum or-

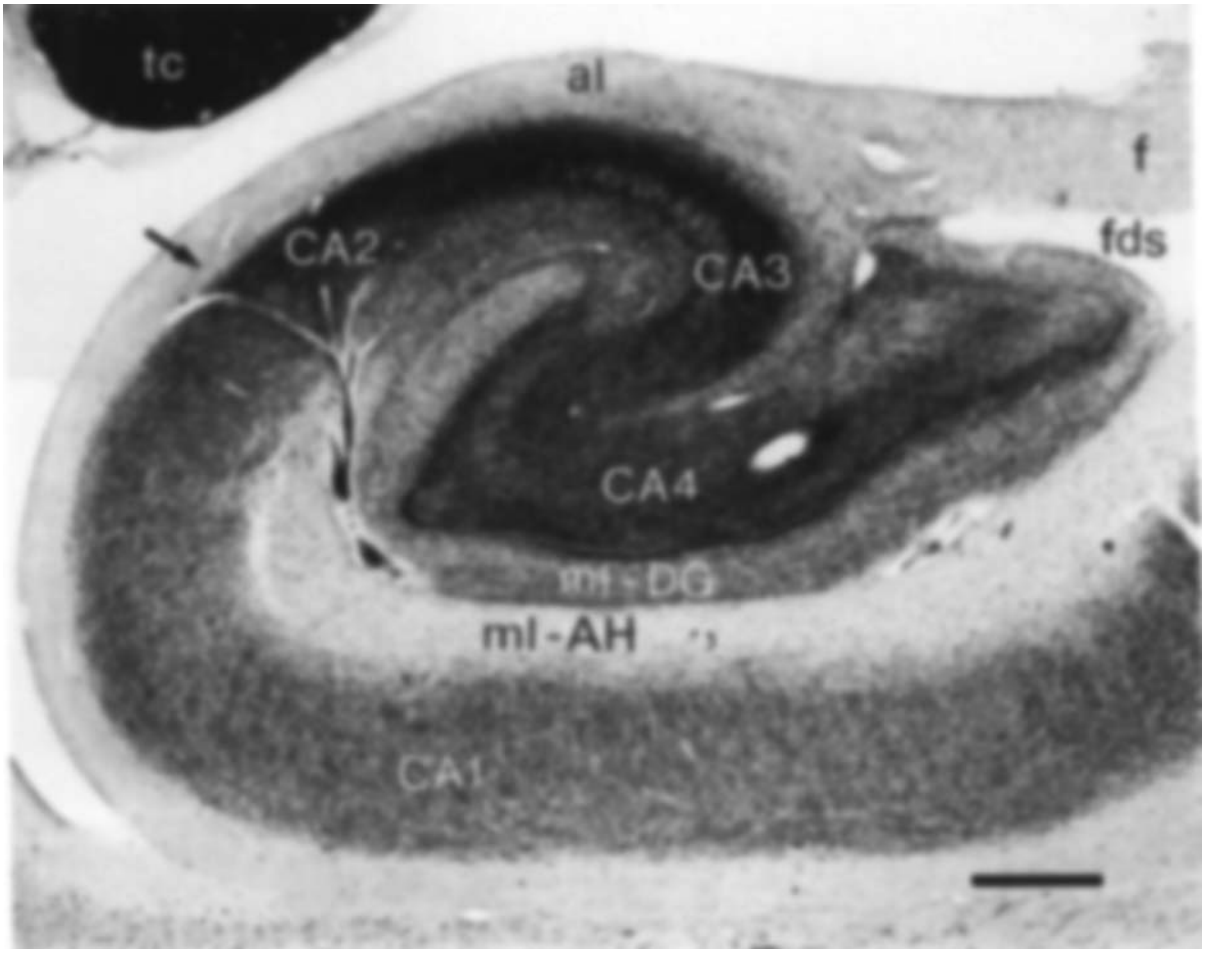

Fig. 3. This brightfield photomicrograph of an AChE stained and lightly Nissl counterstained mid-caudal coronal section through the hippocampal formation of a 13-year-old human shows the general distribution of AChE staining. The heaviest AChE staining occurs within the pyramidal cell layer of the CA2-4 regions and within a thin band along the inner edge of the ml-DG. The arrow indicates a change in AChE staining, which may represent the boundary between CA2 and CA1.

iens, stratum pyramidale, stratum lucidum (or layer of mossy fibers), stratum radiatum, and stratum lacunosum-moleculare (Fig. 2). The organization of these laminae is helpful in defining cytoarchitectonic boundaries and transitional zones, as in the transition from CA1 to subiculum, where the stratum radiatum narrows and disappears; and the transition from CA3 to CA2, which is marked by the termination of the stratum lucidum (Fig. 4).

Distribution of AChE. The hilum of the DG reveals an intense and heterogeneous pattern of AChE staining. Within the hilum, distinct layering is not seen, but there are broad areas of lesser and greater staining intensity within CA4 and the polymorphic layer of the dentate complex (Fig. 4). Among the CA sectors, CA2 and CA3 are the most heavily stained (Fig. 3,4).

The AChE intensity also varies according to the vertical laminae. The alveus is largely unstained, although short segments of individual AChE-positive fibers may be seen to be running through this layer. The stratum oriens is located between the alveus and the stratum pyramidale and contains loosely packed polymorphic cells, many of which stain strongly for AChE. In the CA3 and CA2 sectors, intense AChE staining is seen over the stratum pyramidale and the stratum oriens, forming a heavy band that becomes less intense throughout the CA1 sector. Stratum radiatum is moderately stained in the CA3 region and becomes progressively lighter through the subsequent sectors until both staining and layer disappear altogether at the transition to subiculum. The stratum lacunosum-moleculare is relatively less intensely stained, but like the alveus has numerous individual AChE-positive fibers running throughout it (Fig. 4). Between the stratum pyramidale and the stratum radiatum of the CA3 regions is the layer of mossy fibers (stratum lucidum). Within this band there is less AChE staining than in the adjacent strata. AChE-positive fibers perpendicular to the mossy fibers cross the stratum lucidum (Fig. 4).

The subicular complex

Nomenclature. The subicular complex is located between Ammon's horn on one side and the entorhinal region on the other, and is made up of the subiculum, the presubiculum, and the parasubiculum. In the primate, the subiculum is the major source of efferent fibers from the hippocampal formation to other parts of the cerebral cortex and to the mammillary bodies (Rosene and Van Hoesen,

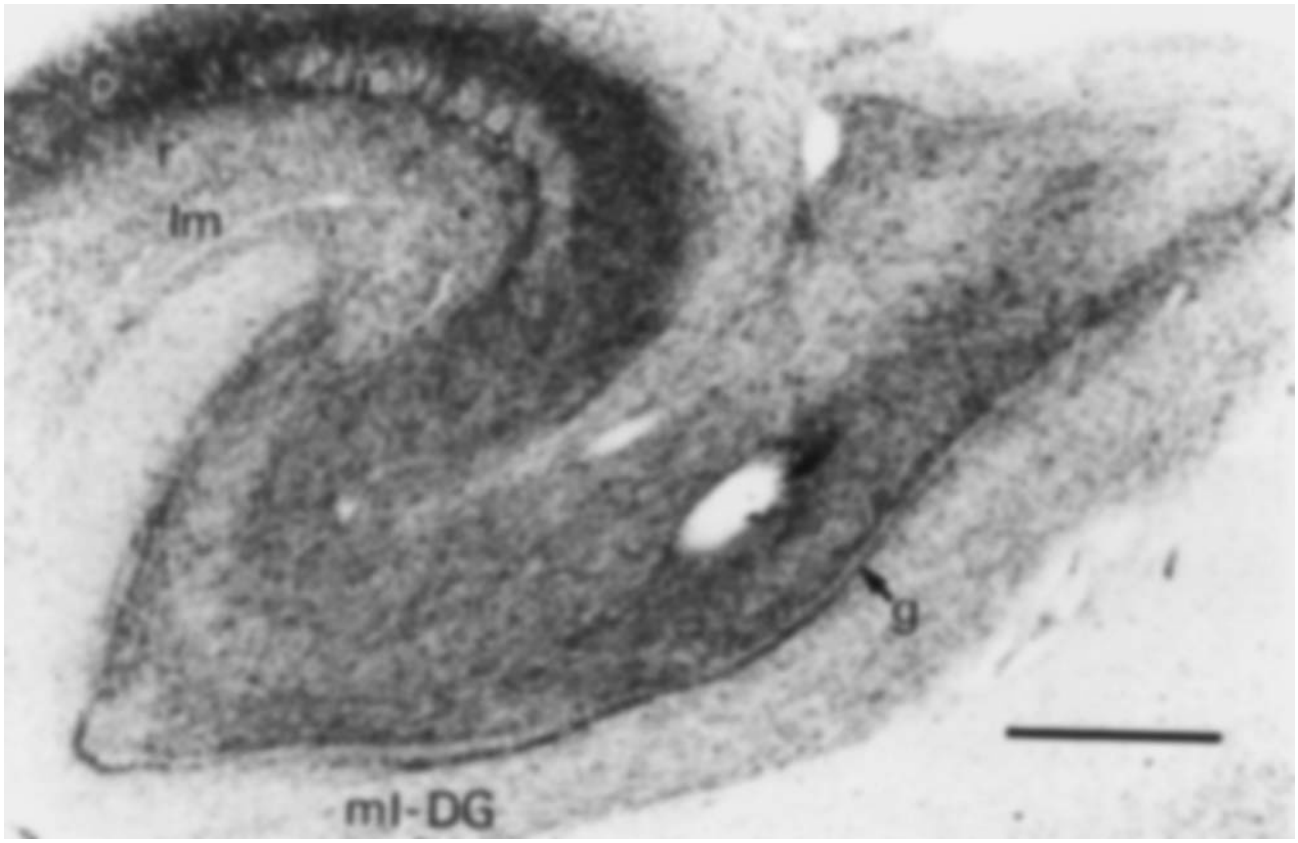

Fig. 4. This is a higher powered view of the same section shown in Figure 3. The stratum lucidum (mossy fiber layer) stains lightly for AChE, but there are a number of intensely stained fibers that cross perpendicular to the mossy fibers. Polymorphic cells within the hilum of the dentate gyrus are AChE-rich but cannot be discerned clearly at this magnification. Calibration mark = 1 mm.

'77; Schwerdtfeger, '79). The human subiculum has been described as the refined magnocellular core of the hippocampus (Braak, '80). It is characterized by a complex lamination pattern with local variations that reflect architectonic transitional zones with adjacent sectors.

The transition from Ammon's horn to the subiculum is marked by the extension of a band of superficial CA1 neurons (Figs. 1, 5). This band of cells gradually narrows as it protrudes from the Ammonic region, forming a diagonal boundary. Subjacent to the extended finger of CA1 pyramidal cells are the subicular pyramids. The external and internal laminae together form the pyramidal layer of the subiculum, which expands as the overlying CA1 neurons narrow and disappear.

Overlying the human subiculum, distinctive "clouds" of small, moderately Nissl stained and densely packed neurons appear (Figs. 1, 6, 7A). This formation represents the beginning of the presubiculum. Moving away from the Ammonic region, these islands of cells appear to coalesce, forming the main body of the superficial layer of the presubiculum. Like the subiculum, the presubiculum has a more densely packed superficial layer and a more loosely aggregated subjacent layer.

The presubiculum overlies the subiculum itself and continues away from the Ammonic region until it meets layers II and III of the entorhinal cortex (Figs. 1, 6). A modest parasubicular region is interposed within the lateral transition from presubiculum to entorhinal cortex. The parasubiculum is a relatively prominent structure in the monkey brain, but in the human it is less notable, appearing as an inconspicuous wedge-shaped collection of variably sized cells (which are generally larger than the presubicular cells) at the tip of the parahippocampal gyrus. The boundary between the subiculum and the entorhinal cortex is not distinct, but the transition occurs where the subicular pyramids merge into those of the deeper layers of entorhinal cortex (Figs. 1, 6).

Distribution of AChE. The moderately heavy AChE staining seen in the CA1 pyramidal cell layer is also present in the finger of superficial CA1 pyramids, which forms the transitional zone between CA1 and the subiculum (Fig. 5). In some sections, this transitional area appears to be slightly more heavily stained than the adjacent CA1 region and the AChE positive fibers form a diagonal band that further highlights the cytoarchitectonic transition. The subiculum itself is more lightly stained and AChE staining does not distinguish between the external and internal pyramidal layers (Fig. 5).

The presubicular "clouds" within the molecular layer overlying the subiculum are each invested by a web of

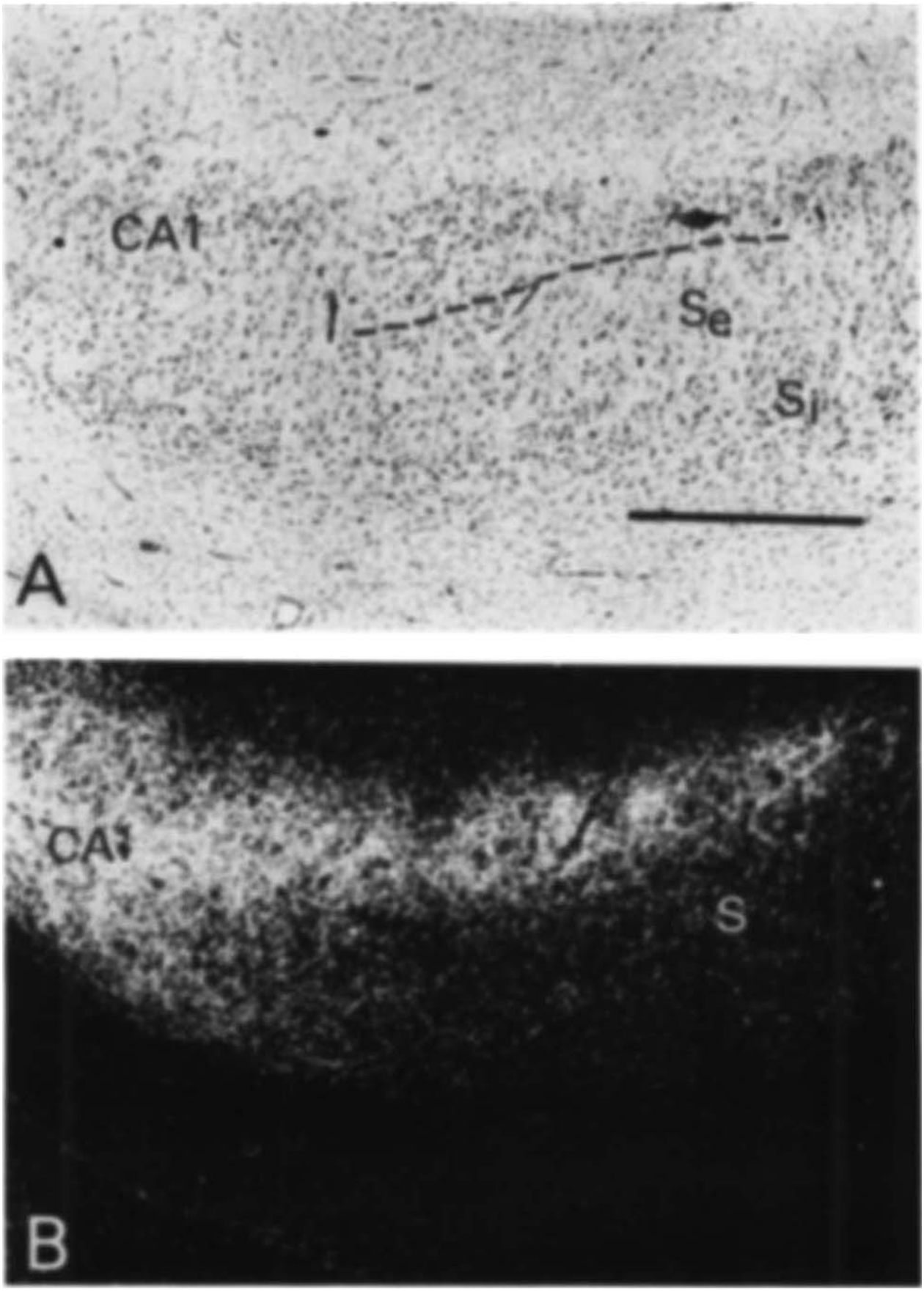

Figure 5

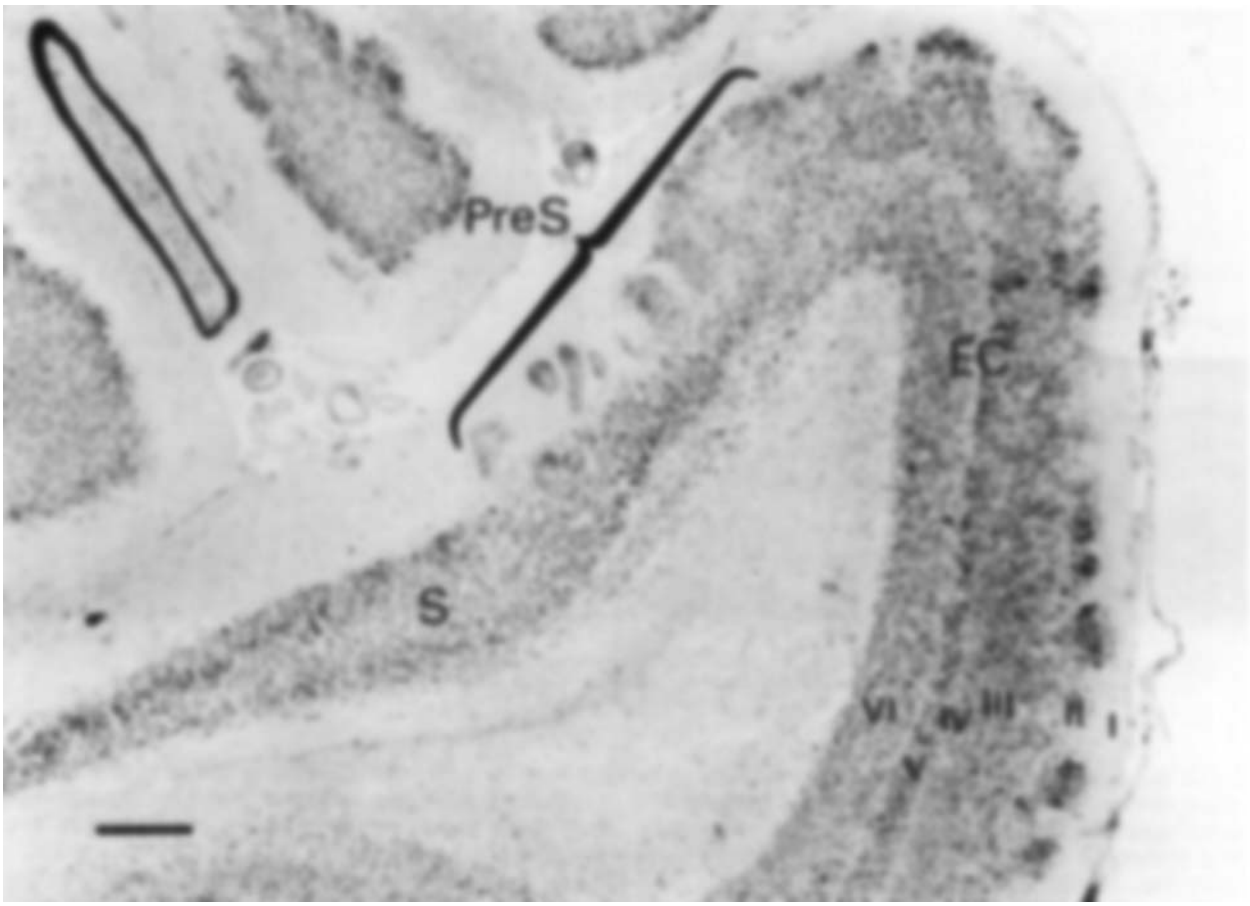

Fig. 6. This celloidin embedded, Nissl-stained section of the parahippocampal gyrus shows the architectonic structure of the EC from a 43-year-old human. The PreS includes both the "clouds" of smaller cells and the confluence of these cells as one moves laterally toward the EC. Calibration mark = 1 mm.

AChE positive fibers (Fig. 7B). The remainder of the presubiculum demonstrates moderate AChE staining in the more densely packed superficial layer, and light AChE staining throughout the underlying deeper layer. AChE staining does not help to delineate the parasubiculum from the adjacent presubiculum.

The entorhinal cortex

Nomenclature. The layers of the entorhinal cortex (EC) as designated in the human (Brodmann, '09) and the monkey (Van Hoesen and Pandya, '75a; Amaral et al., '83) are easily recognized, and we have preserved this 6-layered nomenclature (Figs. 1, 6). With Nissl staining, layer I (outer plexiform zone) is a wide cell-sparse layer. Layer II contains large stellate cells, which may be aggregated into small clumps. Layer III is wider and consists of medium-size pyramidal cells. Layer IV (inner plexiform layer or lamina dissecans) is a narrow, cell-sparse layer. Layer V includes a more darkly staining, narrow band of smaller pyramidal cells, whereas layer VI is a broader, multilaminated band of polymorphic and spindle-shaped cells (Van Hoesen and Pandya, '75a).

In the monkey, the "lateral" entorhinal cortex, or area 28b, lies rostral to the "medial" entorhinal cortex, or area 28a, and an intermediate region (28i) has been proposed as a transitional region between the two (Van Hoesen and Pandya, '75a). As one moves caudally through the monkey EC, the transition from 28b to 28a is characterized by closer alignment of the patches in layer II, a more distinct layer IV, and sharper lamination of VI. In the human, the difference between the rostral and caudal patterns of the entorhinal cortex is less clear-cut, principally because layer II remains patchy throughout most of its rostral-caudal extent and because layer IV is relatively distinct throughout the rostral-caudal course.

The prominent clumps of stellate cells in layer II of the human EC become less patchy and less darkly staining along the medial bank of the rhinal sulcus (Fig. 1). This cortex has been distinguished as the prorhinal cortex (Filimonov, '49, as cited in Van Hoesen and Pandya, '75a) in the monkey and has been treated as a gradual transitional zone between allocortex and isocortex in human studies (Economo and Koskinas, '25). The prorhinal cortex merges with area 35 or perirhinal cortex at the fundus of the rhinal

Fig. 5. These are adjacent coronal sections through the mid-caudal hippocampus of a 30-year-old human. The first is stained with Nissl (**A**), whereas **B** is stained with AChE and photographed with darkfield optics. The transition between CA1 and subiculum is delimited by a finger of more darkly staining CA1 neurons, which overlap with the subiculum. This border between CA1 and subiculum demonstrates a marked difference in the AChE staining of the two sectors. Calibration mark = 1 mm.

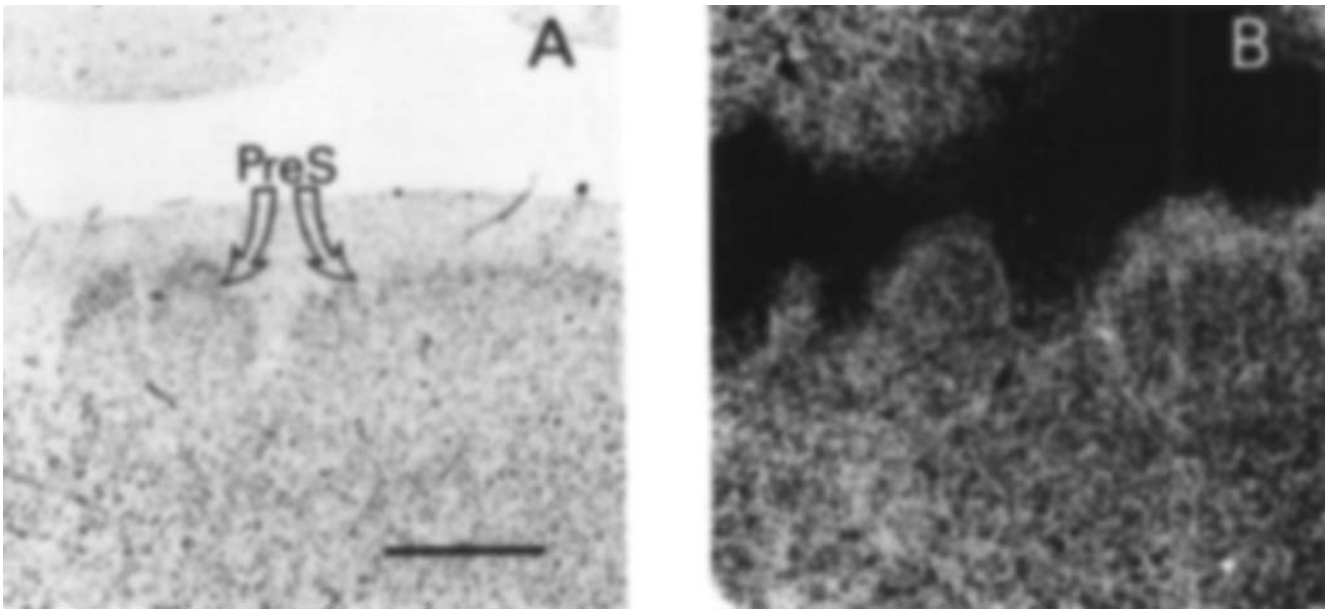

Fig. 7. Adjacent coronal sections through the rostral hippocampus of a 13-year-old human are stained for Nissl (A) and AChE (B). The darkfield photomicrograph (B) demonstrates AChE positive fibers that invest the small "clouds" of cells in the presubiculum. Calibration mark = 500 μm.

sulcus of the monkey (Brodmann, '09) and has been characterized in that species as an intermediate type of cortex (proisocortex), which forms a transition between periallocortical entorhinal cortex medially and temporal neocortex laterally (Van Hoesen and Pandya, '75a).

Distribution of AChE. All AChE staining in the human EC is generally lighter than the staining found in the hippocampal complex, but slightly more prominant than the very light staining found in the adjacent temporal isocortex (Fig. 8). Human EC demonstrates distinctive banding that corresponds to the laminar cytoarchitectonic features (Fig. 8).

The most prominent AChE staining in the human EC occurs in two bands: one corresponding to layer II and a second corresponding to layer IV-V. Examination of counterstained material reveals that the areas of AChE positivity in layer II are made up of fibers overlying the islands of stellate cells and extending slightly into the molecular layer. The second prominent band of AChE fiber staining is distributed most densely throughout layer IV and extends as well into the superficial portion of layer V.

Along the medial bank and toward the fundus of the rhinal sulcus, the AChE staining in layer II loses its patchiness and becomes less intense. The most prominent AChE fiber staining in this sulcal zone is characterized by a band of staining that slopes obliquely away from layer II until it joins an intermediate pyramidal cell layer (Fig. 8).

Some comparisons with AChE staining in the monkey

Comparison of AChE staining in the human and monkey hippocampus reveals many similarities and several notable differences (Figs. 4, 9). The most dramatic difference is in the AChE staining of the molecular layer of the dentate gyrus (ml-DG). In the monkey there is an intensely AChE-staining band throughout the inner one-third of the ml-DG; whereas in the human there is only a very thin layer of staining immediately adjacent to the granular cell layer. Another conspicuous difference involves the parasubiculum, which in the monkey is clearly demarcated by intense AChE staining (see Figs. 9, 12 in Bakst and Amaral, '84). In the corresponding part of the human parahippocampal region, it is difficult to distinguish an analogous area of relatively more intense AChE staining.

DISCUSSION

We have described the AChE distribution in the human hippocampus and parahippocampal gyrus, confirming and extending previous brief descriptions (Friede '66; Mellgren et al., '77; Kelovic and Kostovic, '81). As described in the rat (Storm-Mathisen and Blackstad, '64), the guinea pig (Geneser-Jensen and Blackstad, '71; Geneser-Jensen, '72a,b), the monkey (Bakst and Amaral, '84), and the rabbit (Geneser, '86), the human hippocampal complex has a distinctive distribution of AChE fibers that varies from region to region.

The distribution of AChE fibers in the monkey is similar in most respects to that in the human. The monkey also has prominent AChE-rich polymorphic neurons within the hilum, although these can be difficult to discern beneath the heavy CA4 fiber staining. However, in the monkey there is a dense band of heavily staining AChE corresponding to the inner third of the molecular layer, with less intense staining throughout the remainder of the molecular layer. In the human, the band of heavy AChE staining along the inner edge of the molecular layer is considerably thinner. In the rat, the AChE-rich band in the ml-DG is one of the major recipient zones for the cholinergic septohippocampal projection (Lewis and Shute, '67). The more external layers of the ml-DG in both the rat (Steward, '76) and the monkey (Van Hoesen et al., '72) receive entorhinal projections through the perforant pathway. If this arrangement is also found in humans, the interspecies difference in the relative width of the AChE-rich band could indicate

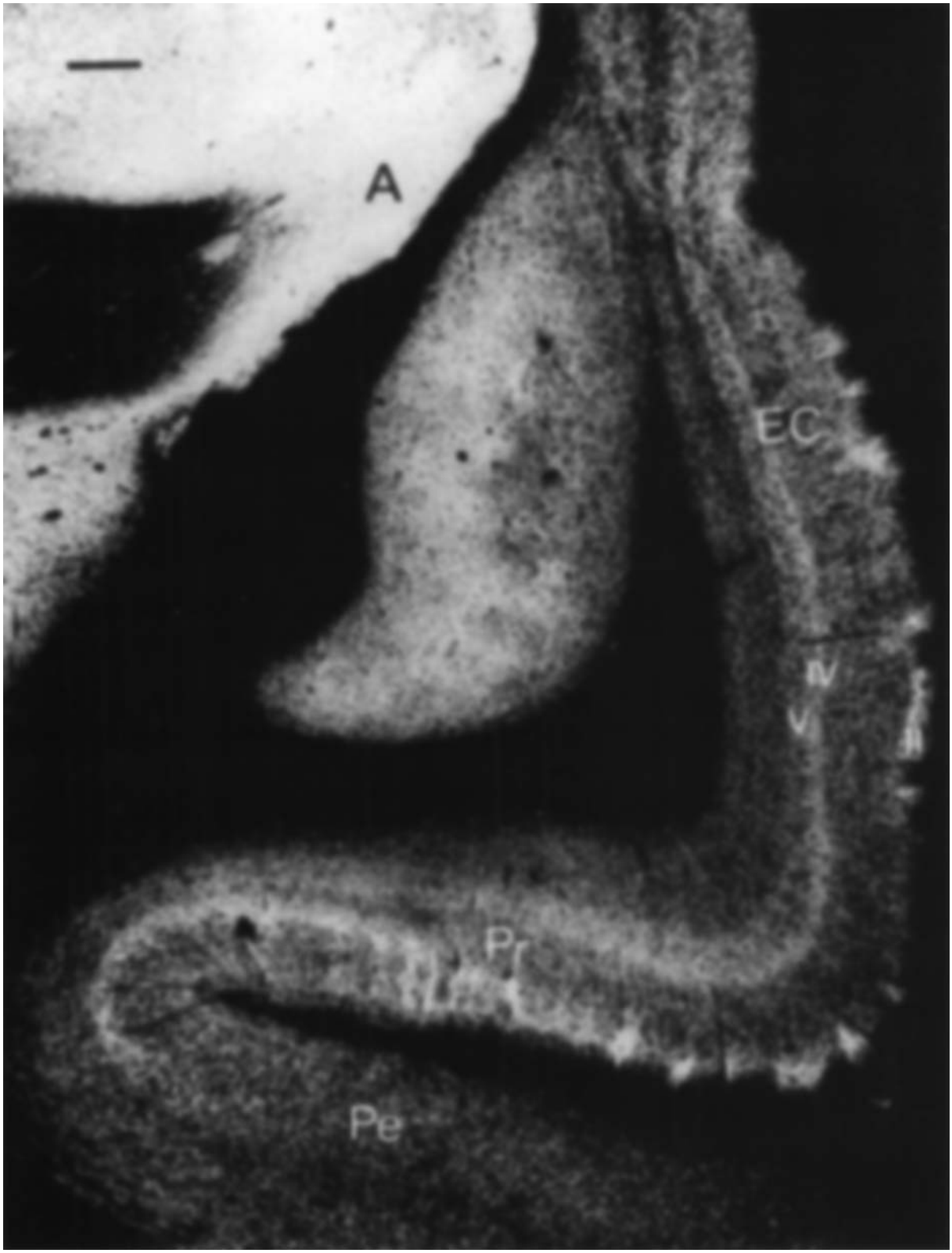

Fig. 8. This is a low power, darkfield photomicrograph of an AChE-stained coronal section through the amygdala and rostral tip of the hippocampus. Note the laminar distribution of AChE in the EC and the changes at the start of the rhinal sulcus where the prominent band of staining in layer II apears to slope obliquely away from the surface. The lateral bank of the rhinal sulcus is relatively more lightly stained. The rostral tip of the hippocampus and the amygdala (Herzog and Kemper, '80; Svendsen and Bird, '85) stain heavily. Calibration mark = 1 mm.

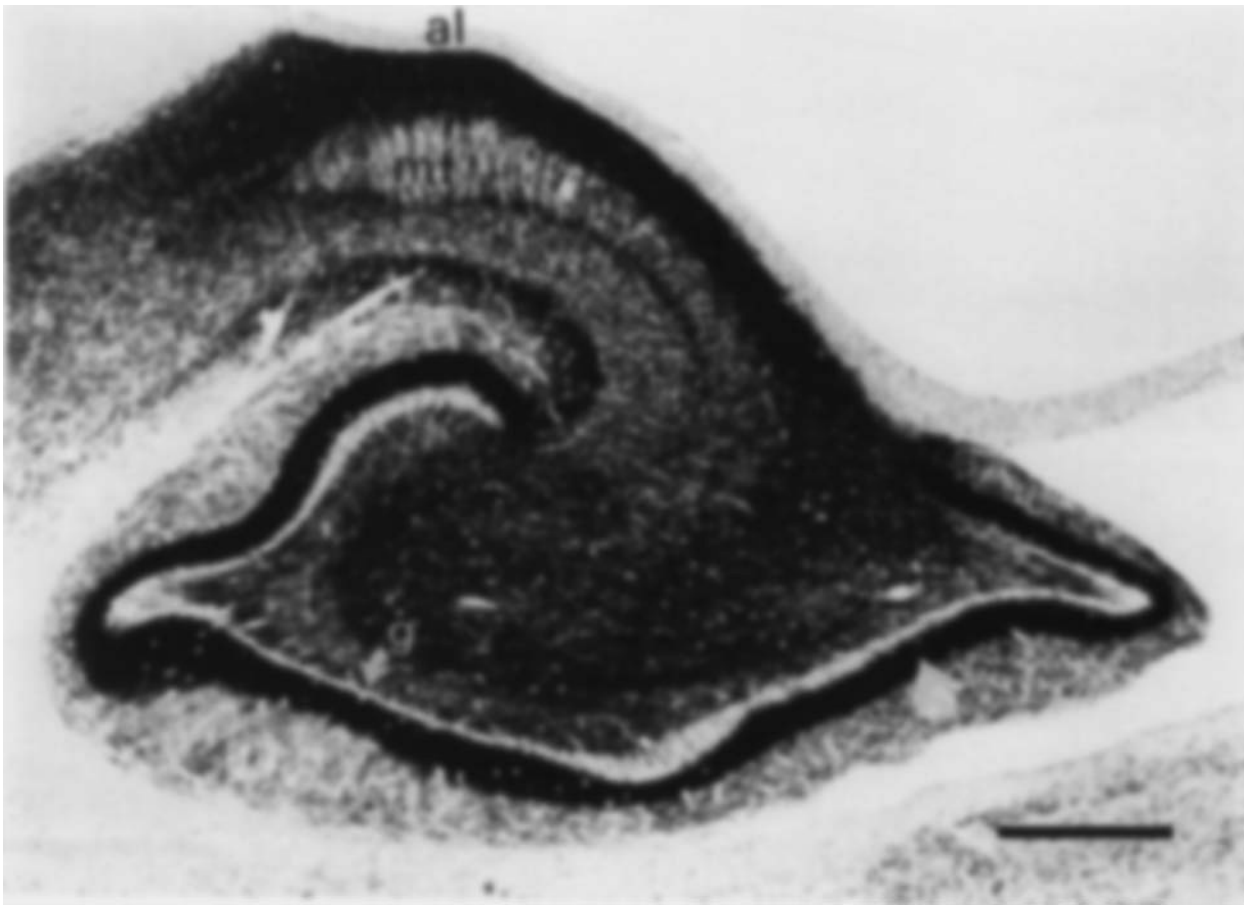

Fig. 9. This is an AChE-stained coronal section from the hippocampus of a rhesus monkey. The monkey ml-DG (large arrow) has a wide AChE-rich band along its inner third. Human AChE staining is very similar to that of the monkey except for the lesser width of the AChE-rich band. Calibration mark = 1 mm.

that the ratio of entorhinal to septal ml-DG afferents is higher in the human brain than in the monkey.

The cytoarchitectonic boundary between CA1 and the subiculum takes place along a diagonal finger of superficial CA1 cells (Braak, '80). This feature may be seen in the monkey as well (Figs. 1, 2A in Bakst and Amaral, '84). At this transitional region in both monkey and human, there is a band of relatively increased AChE staining that parallels the extension of CA1 neurons. Although this feature is less conspicuous in the human brain, this diagonal region interspersed between CA1 and the subiculum may correspond to the prosubiculum of the monkey (Van Hoesen and Pandya, '75c).

The human presubiculum is more extensive than in the monkey, and in the human there are distinctive clumps or "clouds" of cells that overlie the subiculum. In the human brain the most prominent AChE staining in the presubiculum is associated with fibers surrounding, and to a lesser degree, interdigitating with these superficial small cells. The description of AChE distribution in the human presubiculum finds some parallels in the report by Geneser-Jensen and Blackstad ('71), which appears to demonstrate relatively light staining among the presubicular cells of the guinea pig with a surrounding region of heavier staining.

Our observations of the AChE fiber distribution in the human entorhinal cortex confirm those reported by Kelovic and Kostovic ('81). They noted "patches" of AChE staining in layers I and II that corresponded to the cell islands in layer II and extended beyond them into layer I. They also noted that when the "patches" were traced from section to section, they were seen to be bands of AChE positivity that extended in the anteroposterior direction, and they suggested that such bands represented loci of afferent input to the entorhinal cortex.

As the entorhinal cortex makes the transition to the temporal isocortex, the islands of hyperchromic layer II cells coalesce at the superior lip of the rhinal sulcus. A continuation of this layer appears to run obliquely through the cortex along the superior bank of the rhinal sulcus and to merge with the pyramidal cells of layer III. This parallels the pigmentoarchitectonic patterns observed by Braak ('80), who described this area as the "transentorhinal subregion." The AChE pattern we have described shows a similar coalescence of patchy staining and an AChE-rich band that slopes away from the cortical surface to become parallel to the surface again at a deeper level. This region, with its distinctive cytoarchitecture and AChE fiber pattern, corresponds to the prorhinal cortex as described in the

monkey (Van Hoesen and Pandya, '75a).

The AChE pattern along the lateral bank of the rhinal sulcus is lighter than in the more medial allocortical and periallocortical areas. In the monkey, paralimbic regions such as the insula, caudal orbitofrontal cortex, the temporal pole, and the parahippocampal gyrus receive a heavier cholinergic innervation than adjacent association cortex (Mesulam et al., '86). Our observations in the parahippocampal region suggest that a similar pattern may also exist in the human brain.

ACKNOWLEDGMENTS

We thank Dr. Anna Sotrel (neuropathologist at Beth Israel Hospital), Dr. William Q. Sturner and Dr. Kristin Sweeney (of the Rhode Island Medical Examiner's Office), who provided autopsy tissue used in this study, and Dr. Albert Galaburda for providing additional Nissl-stained slides of normal human tissue. We appreciate the excellent technical assistance of Terry Martin and Seth Kupferschmid. This work was supported by the Lennox Fellowship of the American Epilepsy Society (R.C.G.), the McKnight Foundation, and by the NIA (Alzheimer's Disease Research Center).

LITERATURE CITED

Amaral D.G., and F. Eckenstein (1986) An immunohistochemical analysis of the cholinergic innervation of the monkey hippocampal formation using a polyclonal antiserum to choline acetyltransferase. Soc. Neurosci. Abstr. *12:*442.

Amaral, D.G., R. Insausti, and W.M. Cowan (1983) Evidence for a direct projection from the superior temporal gyrus to the entorhinal cortex in the monkey. Brain Res. *275:*263–277.

Babb, T.L., and W.J. Brown (1987) Pathological findings in epilepsy. In J.E. Engel, Jr. (ed): Surgical Treatment of the Epilepsies. New York: Raven Press, pp. 511–540.

Bakst, I., and D.G. Amaral (1984) The distribution of acetylcholinesterase in the hippocampal formation of the monkey. J. Comp. Neurol. *225:*344–371.

Braak, H. (1980) Architectonics of the human telencephalic cortex. Berlin: Springer-Verlag.

Brodman, K. (1909) Vergleichende Lokalisationslehre der Grosshirnrinde in ihren Prinzipien dargestellt auf Grund des Zellenbues. Leipzig: Barth.

Economo, C.V., and G.N. Koskinas (1925) Die Cytoarchitektonik der Hirnrinde des Erwachsenen Menschen. In H. Braack: Aritectonics of the Human Telecephalic Cortex. Berlin: Springer-Verlag.

Fonnum, F. (1970) Topographic and subcellular localization of choline acetyltransferase in the rat hippocampal region. J. Neurochem. *17:*1029–1037.

Friede, R.L. (1966) The histochemical architecture of the Ammon's horn as related to its selective vulnerability. Acta Neuropath. *6:*1–13.

Geddes, J.W., D.T. Monaghan, C.W. Cotman, I.T. Lott, R.C. Kim, and H.C. Chui (1985) Plasticity of hippocampal circuitry in Alzheimer's disease. Science *230:*1179–1181.

Geneser, F.A. (1986) Distribution of acetylcholinesterase in the hippocampal region of the rabbit. I. Entorhinal area, parasubiculum and presubiculum. J. Comp. Neurol. *254:*352–368.

Geneser-Jensen, F.A. (1972a) Distribution of acetyl cholinesterase in the hippocampal region of the guinea pig. II. Subiculum and hippocampus. Z. Zellforsch. *1244:*546–560.

Geneser-Jensen, F.A. (1972b) Distribution of acetyl cholinesterase in the hippocampal region of the guinea pig. III. The dentate area. Z. Zellforsch. *131:*481–495.

Geneser-Jensen, F.A. and T.W. Blackstad (1971) Distribution of acetyl cholinesterase in the hippocampal region of the guinea pig. I. Entorhinal area, parasubiculum, and presubiculum. Z. Zellforsch. *114:*460–481.

Herzog, A.G. and T.L. Kemper (1980) Amygdaloid changes in aging and dementia. Arch. Neurol. *37:*625–629.

Horel, J.A. (1978) The neuroanatomy of amnesia. Brain *101:*403–445.

Hyman B.T., L.J. Kromer, and G.W. Van Hoesen (1987) Reinnervation of the hippocampal perforant pathway zone in Alzheimer's disease. Ann. Neurol. *21:*259–267.

Hyman, B.T., G.W. Van Hoesen, A.R. Damasio, and C.L. Barnes (1986) Alzheimer's disease: cell-specific pathology isolates the hippocampal formation. Science *225:*1168–1170.

Kelovic, Z., and I. Kostovic (1981) Banding pattern in human entorhinal cortex revealed by acetylcholinesterase histochemistry. Anat. Rec. *199:*135A.

Kemper, T.L. (1984) Neuroanatomical and neuropathological changes in normal aging and in dementia. In Albert M.L. (ed): Clinical Neurology of Aging. New York: Oxford University Press.

Koelle G.B., and J.S. Friedenwald (1949) A histochemical method for localizing cholinesterase activity. Proc. Soc. Exp. Biol. *70:*617–622.

Lewis, P.R., and C.C.D. Shute (1967) The cholinergic limbic system: Projections to hippocampal formation, medial cortex, nuclei of the ascending cholinergic reticular system, and the subfornical organ and supraoptic crest. Brain *90:*521–542.

Lorente de Nó, R. (1934) Studies on the structure of the cerebral cortex. II Continuation of the study of the ammonic system. J. Psychol. Neurol. *46:*113–177.

Matthews, D.A., P.M. Salvaterra, G.D. Crawford, C.K. Hauser, and J.E. Vaughn (1983) Distribution of choline acetyltransferase positive neurons and terminals in hippocampus. Soc. Neurosci. Abstr. *9:*79.

Mathisen, J.S., and T.W. Blackstad (1964) Cholinesterase in the hippocampal region. Acta Anat. *54:*216–253.

Mellgren S.I. (1973) Distribution of acetylcholinesterase in the hippocampal region of the rat during postnatal development. Z. Zellforsch. *141:*375–400.

Mellgren, S.I., and B. Srebro (1973) Changes in acetylcholinesterase and distribution of degenerating fibers in the hippocampal region after septal lesions in the rat. Brain Res. *52:*19–36.

Mellgren, S.I., W. Harkmark, and B. Srebro (1977) Some enzyme histochemical characteristics of the human hippocampus. Cell Tiss. Res. *181:*459–471.

Mesulam, M-M., A. Rosen and E.J. Mufson (1984) Regional variations in cortical cholinergic innervation: Chemoarchitectonics of acetylcholinesterase-containing fibers in the macaque brain. Brain Res. *311:*245–258.

Mesulam, M.-M., L. Volicer, J.K. Marquis, E.J. Mufson, and R.C. Green (1986) Systematic regional difference in the cholinergic innervation of the primate cerebral cortex: Distribution of enzyme activities and some behavioral implications. Ann. Neurol. *19:*144–151.

Okinaka, S., M. Yoshikawa, M. Uono, T. Muro, T. Mozai, A. Igata, H. Tanabe, S. Ueda, and M. Tomonaga (1961) Distribution of cholinesterase activity in the human cerebral cortex. Amer. J. Phys. Med. *40:*135–145.

Ramón y Cajal, S.R. The structure of Ammon's Horn. (1893, reprinted 1968) Springfield: Charles Thomas.

Rosene D.L., and G.W. Van Hoesen (1977) Hippocampal efferents reach widespread areas of cerebral cortex and amygdala in the rhesus monkey. Science *198:*315–317.

Schwerdtfeger, W.K. (1979) Direct efferent and afferent connections of the hippocampus with the neocortex in the marmoset monkey. Am. J. Anat. *156:*77–82.

Squire, L.R. (1986) Mechanisms of memory. Science *232:*1612–1619.

Svendsen C.N., and E.D. Bird (1985) Acetylcholinesterase staining of the human amygdala. Neurosci. Lett. *54:*313–318.

Stephan, H. (1983) Evolutionary trends in limbic structures. Neurosci. Biobehav. Rev. *7:*367–374.

Steward, O. (1976) Topographic organization of the projections from the entorhinal area to the hippocampal formation of the rat. J. Comp. Neurol. *167:*285–314.

Terry R, and R. Katzman (1983) Senile dementia of the Alzheimer type: defining a disease. In: Katzman R. and R. Terry (eds.): Neurology of Aging. Philadelphia: F.A. Davis, pp. 51–84.

Van Hoesen, G.W., and D.N. Pandya (1975a) Some connections of the entorhinal area (area 28) and perirhinal area (area 35) cortices of the rhesus monkey. I. Temporal lobe afferents. Brain Res. *95:*1–24.

Van Hoesen, G.W., and D.N. Pandya (1975b) Some connections of the entorhinal area (area 28) and perirhinal area (area 35) cortices of the rhesus monkey. II. Frontal lobe afferents. Brain Res. *95:*25–38.

Van Hoesen, G.W., and D.N. Pandya (1975c) Some connections of the entorhinal area (area 28) and perirhinal area (area 35) cortices of the rhesus monkey. III. Efferent connections. Brain Res. *95:*39–59.

Vijayan, V.K. (1979) Distribution of cholinergic neurotransmitter enzymes in the hippocampus and the dentate gyrus of the adult and the developing mouse. Neuroscience *4:*121–137.

Yakovlev, P.I. (1970) Whole brain serial histological sections. In C.G. Tedeschi (ed): Neuropathology: Methods and Diagnosis. Boston: Little, Brown, pp. 371–378.

Zola-Morgan, S., L.R. Squire, and D.G. Amaral (1986) Human amnesia and the medial temporal region: Enduring memory impairment following a bilateral lesion limited to field CA1 of the hippocampus. J. Neurosci. *6:*2950–2967.